

Received March 5, 2019, accepted March 17, 2019, date of publication April 1, 2019, date of current version April 17, 2019.

Digital Object Identifier 10.1109/ACCESS.2019.2907984

Robust Inter-Vehicle Distance Estimation Method Based on Monocular Vision

LIQIN HUANG¹, TING ZHE¹, JUNYI WU¹,

QIANG WU², (Senior Member, IEEE),

CHENHAO PEI¹, AND DAN CHEN¹

¹College of Physics and Information Engineering, Fuzhou University, Fuzhou 350108, China

²School of Electrical and Data Engineering, University of Technology Sydney, Sydney, NSW 2007, Australia

Corresponding author: Dan Chen (cd@fzu.edu.cn)

This work was supported by the Major Science and Technology Projects in Fujian, China, under Grant 2018H0018.

ABSTRACT Advanced driver assistance systems (ADAS) based on monocular vision are rapidly becoming a popular research subject. In ADAS, inter-vehicle distance estimation from an in-car camera based on monocular vision is critical. At present, related methods based on a monocular vision for measuring the absolute distance of vehicles ahead experience accuracy problems in terms of the ranging result, which is low, and the deviation of the ranging result between different types of vehicles, which is large and easily affected by a change in the attitude angle. To improve the robustness of a distance estimation system, an improved method for estimating the distance of a monocular vision vehicle based on the detection and segmentation of the target vehicle is proposed in this paper to address the vehicle attitude angle problem. The angle regression model (ARN) is used to obtain the attitude angle information of the target vehicle. The dimension estimation network determines the actual dimensions of the target vehicle. Then, a 2D base vector geometric model is designed in accordance with the image analytic geometric principle to accurately recover the back area of the target vehicle. Lastly, area-distance modeling based on the principle of camera projection is performed to estimate distance. The experimental results on the real-world computer vision benchmark, KITTI, indicate that our approach achieves superior performance compared with other existing published methods for different types of vehicles (including front and sideway vehicles).

INDEX TERMS Attitude angle information, distance estimation, instance segmentation, monocular vision.

I. INTRODUCTION

Research on advanced driver assistance systems (ADAS) is developing rapidly. ADAS play an important role in reducing traffic accidents, preventing rear-end collisions between vehicles [35], and improving traffic safety performance. Inter-vehicle distance estimation is a crucial part of ADAS. Distance estimation methods can be divided into two major classes: sensor-based [9], [12] and vision-based [10], [21] systems. Sensor-based systems use sensors, such as RADAR and LIDAR [19], to accurately provide the distance information of a target vehicle. However, high cost and target vehicle data collection remain as critical issues. Meanwhile, vision-based systems are typically divided into two classes: stereo vision [13], [27] and monocular vision [11], [15]. Stereo vision can more intuitively and accurately calculate

the long distance of vehicles ahead. However, due to the calibration and matching between two cameras, stereo vision systems require a long execution time and exhibit low efficiency and considerable computational complexity. Monocular vision can tolerate a complicated algorithm and can obtain an optimal result within a shorter time than stereo vision [37]. However, the current distance estimation method for monocular vision still experiences problems, such as low precision and a narrow application range. A monocular-vision-assisted driving system can efficiently control real-time performance because it conforms to the human visual system. Moreover, it adapts to the applicable scene of modern vehicles and demonstrates considerable development prospects compared with other systems. Consequently, inter-vehicle distance estimation based on monocular vision has become a popular research topic.

To satisfy the requirements of monocular-vision-assisted driving system positioning, many distance estimation

The associate editor coordinating the review of this manuscript and approving it for publication was Mehul S Raval.

methods based on monocular vision have been proposed recently. On the basis of their experimental results, monocular visual distance estimation methods can be approximately divided into relative depth and absolute distance estimations. Relative depth estimation [22], [23] mostly predicts the depth of each pixel in an image, expresses the foreground and background through different gray values, and finally outputs the depth map of the depth variation of the entire scene. However, several articles, such as [24], have reported that this type of method primarily restores the relative relationship between the target vehicle and the subject vehicle but does not obtain the absolute distance (in meters) of the target vehicle in the scene. A depth map contains redundant information, such as sky, distant buildings, and street trees, which exerts minimal effect on distance measurement in traffic scenarios. Nevertheless, such information will reduce the efficiency of estimating the distance of the target vehicle.

An absolute distance estimation method can obtain the absolute distance of the target vehicle ahead. For absolute distance estimation method, some researches proposed for distance detection using machine learning such as classifier using Haar-like features [14] and cascade classifier [15], [38]. These methods require many positive and negative samples during the training process to ensure good accuracy. However, a satisfactory ranging result cannot be produced. Thereafter, distance estimation based on the geometric model has been proposed. In accordance with different projection principles, distance estimation methods can be further divided into the inverse perspective mapping (IPM) principle and the camera projection principle. In target vehicle distance estimation based on the IPM principle [1], [3], [4], the original image is converted into a bird's eye view via IPM transformation to restore the information of the road plane. Then, the distance of the target vehicle is calculated using the IPM image obtained after the conversion. However, this method has two disadvantages: 1) The image brightness requirement is relatively high. When the acquired image brightness is low, detection system performance is low and distance estimation accuracy is reduced, and 2) The size of the converted image changes, which causes some of the target vehicles in the original image to be lost in the IPM image, thereby limiting the estimated range of the system.

To address the aforementioned problems, a distance estimation method for the vehicle ahead based on the camera projection principle was proposed in [2] using vehicle width estimation and by comprehensively considering two road environments, i.e., with and without lane markings. By detecting the positions of the vehicle ahead [36] and the vanishing point, a method based on the camera projection geometry model was developed in [7] for measuring the longitudinal distance of the vehicle ahead. However, this method cannot obtain detailed information of the target vehicle and acquires redundant information, thereby resulting in low ranging accuracy. Accordingly, a concept based on instance segmentation was proposed in [8] using the projection geometry model established by the projected area to

estimate the distance of the vehicle ahead. Compared with the method presented in [2], [7], redundant information can be reduced and ranging accuracy can be improved. However, no modeling analysis is performed for the mechanism of attitude angle change. The ranging result of the non-front target vehicle exhibits a considerably large error. The application range of the distance estimation method is insufficiently wide. To acquire the actual dimensions of a vehicle, vehicle type is obtained using a vehicle classification network. Then, the actual dimensions of the target vehicle are obtained by matching the dimension information of different types of vehicles that have been previously calculated.

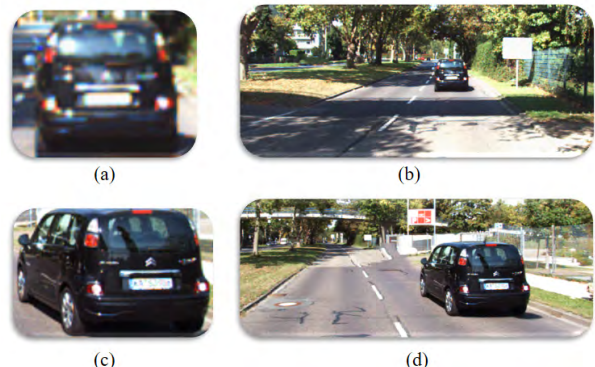


FIGURE 1. (a), (c) Shows partial scene of the vehicle taken along the direction of the camera's optical ray and (b), (d) is the driving situation of the vehicle in whole scene.

Figure 1 shows the change in the attitude angle of the target vehicle when it is in the front and sideway positions of the subject vehicle. As shown in Figs. 1(a) and 1(c), the projection relationship of each part of the vehicle is different, and the corresponding projection information in the image also varies. When the method presented in [8] is used, processing will result in a considerable difference in the accuracy of the distance estimation results among various vehicles, and the accuracy of the overall result will decrease. Therefore, the current study proposes a method based on the monocular vision vehicle distance estimation method by integrating vehicle attitude angle information. To improve the efficiency of a distance estimation system, we enhanced the method for obtaining vehicle dimension information in [8] by applying the advantages of the deep network framework and using the KITTI dataset to train the dimension estimation network and obtain the actual dimensions of a vehicle, thereby improving the detection efficiency of a system.

The rest of this paper is organized as follows. Section II briefly discusses related studies and our contributions, primarily reviewing the progress of previous work in the field of distance estimation research. Section III explains the entire distance estimation system and the method for each block. Section IV introduces the research environment and experimental results to verify the accuracy and robustness of the system. The conclusions of the study and future work are described in Section V.

II. RELATED WORK

In recent years, research on the methods for estimating the distance of monocular vision vehicles based on geometric models, which are largely divided into the inverse perspective mapping transformation method [3], projection geometric relationship method [5], and fitting modeling method [16], has achieved considerable results. In [4], [17], [18], [20], a distance estimation method based on IPM was proposed. The difference among these studies is the object detection method, such as the road removal algorithm [4], [17], threshold adjustment [18], and hue, saturation, and value (HSV) color mapping [20]. The overall idea is to convert the original image into a bird's eye view, which approximates the image obtained from the top-down observation scene. The IPM image obtained through conversion is used to calculate the distance value of the target vehicle. The original image is converted to an IPM image by obtaining the camera's internal and external parameter information. The method is simple and feasible but does not consider the vehicle's attitude angle information when moving, thereby resulting in a considerable distance error when the vehicle moves.

Subsequently, to avoid the problem of conversion between images, [5]–[7] proposed to establish a geometric model based on the principle of camera perspective projection to estimate the distance of the target vehicle. Nakamura *et al.* [5] presented a monocular vision vehicle distance estimation method based on the triangular geometric relationship between the horizontal and vertical directions to estimate vehicle width. However, this method reduces only the error of vehicle width estimation during the tracking process and does not consider the change in the attitude angle produced by the vehicle during driving. Thus, a considerable error in estimating the distance of the non-front target vehicle is produced. Bao and Wang [6] developed a monocular vision ranging method based on the linear relationship between the average vehicle width and the actual distance of the vehicle, however, this method does not consider the attitude change of the vehicle during driving. Moreover, the average width of the vehicle in the image can only guarantee the average ranging accuracy and not the accuracy of the single vehicle ranging result. Huang *et al.* [7] established a method for measuring the longitudinal distance of the target vehicle ahead based on the vanishing point of the lane line by detecting the positions of the vehicle and the vanishing point. The method accurately detects the vanishing point position to ensure the accuracy of the ranging result of the vehicle ahead. However, the deflection of the vehicle during driving is not considered, and this method is applicable only to the front vehicle.

Subsequently, [1] presented a geometric model based on obtaining vehicle position and lane line information while using vehicle height to measure the distance of the vehicle ahead in the modeling of the original and IPM images, thereby solving the information loss problem in image conversion. A distance estimation method based on vehicle

detection information using vehicle width was developed in [2], the method comprehensively considers two road environments, namely, with and without lane markings. However, the methods proposed in [1] and [2] present the position of the target vehicle in the image as rectangular, and thus, many details of the target vehicle cannot be obtained, and a considerable amount of redundant information is included. Huang *et al.* [8] suggested measuring the target vehicle's distance based on vehicle segmentation information using the projected area. Compared with the method that uses vehicle height or width, redundant information can be reduced to improve ranging accuracy. The method developed in [8] disregards the attitude angle problem of a vehicle, and the applicable range of the system has limitations. This method is mostly applicable to front vehicles, whereas the estimation result of sideway vehicles acquires a large error. Moreover, distance estimation by recovering the original projection information of the occluded vehicle from the overlapping area of the rectangle reduces ranging accuracy due to the inaccuracy of the labeling of the rectangle.

In summary, the major contributions of our work are as follows.

- To improve the accuracy of the estimated results and the robustness of the system for vehicles under different driving conditions, This study proposes to integrate vehicle attitude angle information based on vehicle segmentation information to realize distance estimation of the vehicle ahead.
- The 2D base vector geometric model is designed in accordance with the principle of image analytic geometry, and the relationship between the back of the vehicle and the overall projection information of the vehicle is obtained. This relationship is used to determine the projected area of the back of the vehicle.
- The method for obtaining vehicle size information is improved to enhance system efficiency and acquire the actual dimensions of a vehicle through our trained dimension estimation network.
- The test results of the KITTI benchmark dataset show that the error rate for sideway vehicle ranging is less than 5%, and the accuracy deviation among vehicles under different driving conditions is less than 2%. These results considerably narrow the deviation of ranging accuracy among different types of vehicles, overcome the limitations, and exceed the accuracy of existing distance estimation methods.

III. SYSTEM MODEL

A. SYSTEM OVERVIEW

The primary reason for the problem in existing distance estimation methods is that vehicle attitude angle information is not considered. In complex traffic scenarios, the driving conditions of the target vehicle vary relative to the subject vehicle, and the attitude angle information of different types of vehicles and the projection relationship in the image are different. As shown in Fig. 1, the target vehicle moves

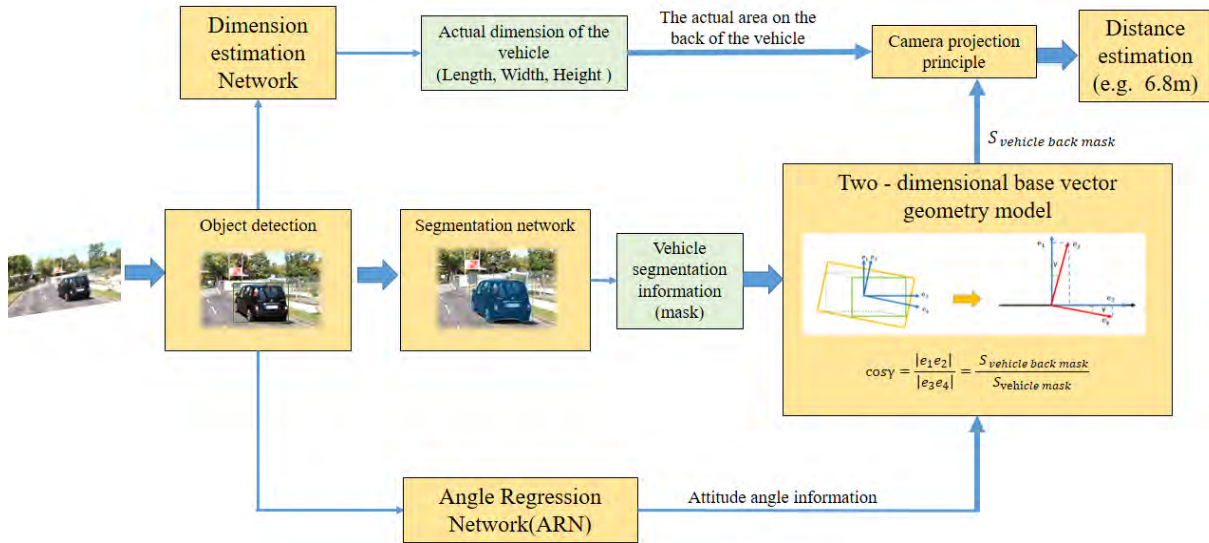


FIGURE 2. Distance estimation system framework.

respectively in the front and sideway positions of the subject vehicle. In the sideway position, the projected parts of the vehicle in the image are not simply formed by the actual back projection of the vehicle, but the front vehicle is formed by the corresponding projection. If the projection relationship is the same, i.e., the projection areas of the two types of vehicles are formed by the back of the vehicle, then the accuracy of the ranging result between the two vehicles deviates considerably, thereby resulting in a decrease in the accuracy of the entire distance estimation system.

In summary, this study considers the vehicle attitude angle information based on a vehicle detection and segmentation algorithm and establishes an “area–distance” geometric model based on the camera projection principle to estimate the distance of the vehicle ahead. The system framework is shown in Fig. 2. First, the entire RGB image is sent to the target detection part to extract the candidate area of the target vehicle. Then, the candidate regions are sent to the segmentation network, ARN, and dimension estimation network to obtain the segmentation information, attitude angle information, and actual dimension of the target vehicle, respectively. Subsequently, a 2D base vector geometric model based on the principle of image analytic geometry [39] is designed to obtain the projection relationship between the back of the vehicle and the entire vehicle, and the projected area of the back of the vehicle is calculated. The angle (γ) is the offset Angle between two pairs of basis vectors in the geometry model, and its physical meaning is the vehicle attitude angle. Lastly, a geometric model based on the camera projection principle is established to estimate the distance of vehicle ahead. In our distance estimation system, a region proposal network (RPN) that combines object classification and object candidate regions is generated. The RPN can be used to

generate the candidate regions of target vehicles, thereby achieving a complete end-to-end target detection module, which not only accelerates detection speed but also improves detection performance. The segmentation network is a pixel-level segmentation of the target vehicle candidate region using the mask region-based convolutional neural network (Mask R-CNN) [25] instance segmentation network to obtain the vehicle mask. Adopting the design ideas and deep network framework of pose estimation in [26], the KITTI dataset was used to train the ARN and dimension estimation network to obtain vehicle attitude angle information and physical dimensions. Subsequently, this section primarily introduces the local module design of the distance estimation system, including the attitude angle design, vehicle back projection information extraction, and distance estimation module design.

B. ATTITUDE ANGLE DESIGN

Given that the driving lane of the subject vehicle changes, the driving position of the target vehicle changes relative to that of the subject vehicle. Thus, the direction of the light between the camera’s optical center and the center of different target vehicles varies, thereby resulting in different attitude angle information of the target vehicles. As shown in Fig. 3, the attitude angle information of a vehicle is transformed into 2D space to establish an analysis plan. The orange rectangular box represents the front vehicle, whereas the blue rectangular box represents the sideway vehicle. The camera’s optical center establishes the camera coordinate system for the origin. The black dotted line indicates the horizontal line of the camera coordinate system, the red arrow indicates the vehicle driving direction, and the blue arrow indicates the light direction. θ_{ray1} and θ_{ray2} are the light ray angles of

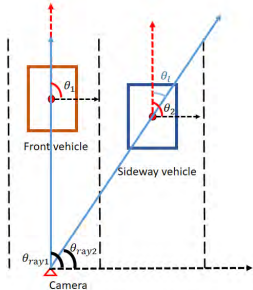


FIGURE 3. Plan of vehicle driving conditions.

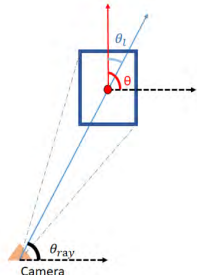


FIGURE 4. Angle geometry relationship.

the front and sideway vehicles, respectively; θ_1 and θ_2 are called the global angles of the front and sideway vehicles, respectively; and θ_l is called the local angle. The local angle of the front vehicle is 0° , whereas the local angle of the sideway vehicle is not 0° . The relationship among angles is shown in Fig. 4. The blue rectangle refers to the target vehicle, the triangle is the camera's optical center of the subject vehicle, and the horizontal dotted line is the horizontal axis of the camera coordinate system. θ_{ray} is the angle between the ray connected to the vehicle center and the optical center and the horizontal axis, θ is the angle between the vehicle driving direction and the horizontal axis, θ_l is the local angle of the vehicle, and $\theta_l = \theta - \theta_{ray}$. Subsequently, θ_{ray} is called the ray angle, θ is called the global angle, and θ_l is called the local angle. Given the change in attitude angle information, the projection relationship and mask information of a vehicle are changed.

To obtain the required attitude angle information, we adopt the concept of rectangular box regression in a Faster R-CNN [34] network and the design idea of the angle estimation architecture in [26]. On the basis of the last layer of the convolution feature map, the regression parameters after the fully connected layers (FC) are modified, the required angle regression network is trained through the KITTI detection dataset, and the attitude angle information is finally obtained. The network structure is shown in Fig. 5.

C. VEHICLE BACK PROJECTION INFORMATION EXTRACTION

This section primarily describes how the projection relationship between the back of the vehicle and the entire vehicle is obtained through attitude angle and segmentation information

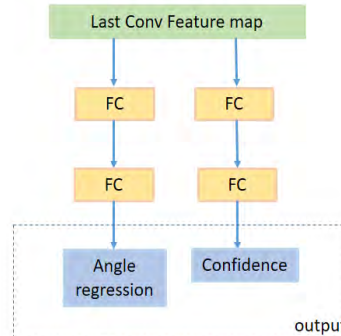


FIGURE 5. Angle regression network structure.

and how the projected area of a vehicle's back is obtained by using this relationship, wherein the pixel value of the mask is obtained from the segmentation information to represent the projected area.

1) RELATIONSHIP BETWEEN THE MASKS OF THE FRONT VEHICLE AND THE BACK OF THE SIDEWAY VEHICLE

We can learn from the Section III-B that vehicle changes under different driving conditions are related to the vehicle attitude angle. Compared with the mask information of the front vehicle, the sideway vehicle also contains other parts of the mask information. However, the back of the vehicle remains unchanged, and the corresponding mask information does not change. Therefore, the projected area on the back of the sideway vehicle is the same as the projected area of the front vehicle, and Equation (1) is obtained.

$$S_{\text{front vehicle mask}} = S_{\text{sideway vehicle back mask}} \quad (1)$$

where $S_{\text{front vehicle mask}}$ is the projected area of the front vehicle and $S_{\text{sideway vehicle back mask}}$ denotes the projected area on the back of the sideway vehicle.

2) RELATIONSHIP BETWEEN THE MASKS OF THE FRONT AND SIDEWAY VEHICLES

Assume that the camera's elevation and roll angles are zero. Then, the image acquired by the camera is parallel to the actual observation scene. In a traffic scene, the vehicle travels on a straight road, regardless of the vehicle driving on the curve.

To obtain the mask on the back of the vehicle, the relationship between the front vehicle mask and the entire mask of the sideway vehicle must be first analyzed. We extract the candidate area of the target vehicle along the direction of the light. As shown in Fig. 6, the area surrounded by the green line indicates the mask projected from the back of the front and sideway vehicles, and the area surrounded by the yellow line indicates the mask of the entire projection of the sideway vehicle.

In accordance with the analytic geometric transformation properties of the 2D image, each planar graph can be represented by a set of linearly independent basis vec-



FIGURE 6. Outline map of target vehicle candidate area, (a) Mask outline of the Front vehicle. (b) Mask outline of Sideway vehicle.

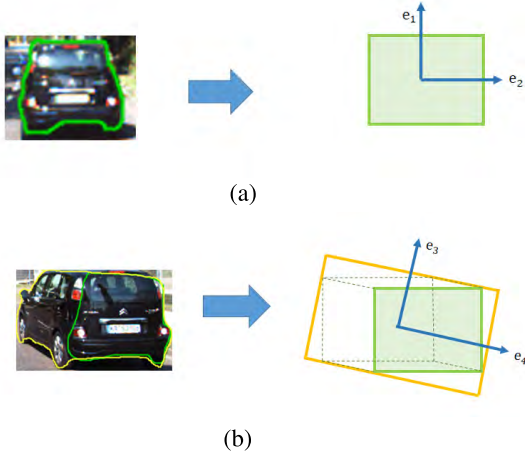


FIGURE 7. Target vehicle contour regularization, The green rectangular frame area approximates the mask on the front vehicle and back of the sideway vehicle, and the yellow rectangle approximates the whole mask of the sideway vehicle. (a) Front vehicle. (b) Sideway vehicle.

tors. Then, the geometric transformation of the figure in the 2D space can also be expressed by the geometric transformation of the base vector. Given that the shape of the mask projected by the vehicle in the image is an irregular pattern, which is inconvenient for further analysis, the rigidity of the vehicle is used to approximate the mask of the vehicle projection using a rectangle.

- The mask of the front vehicle is represented by the e_1-e_2 basis vector, as shown in Fig. 7(a). The target vehicle is extracted along the direction of the camera light. Thus, the physical meaning of the e_1 base vector is the light ray direction of the front vehicle. Given that the direction of the front car is the same as that of the light ray, the e_1 base vector can also represent the driving direction of the vehicle. e_2 is the vertical vector of e_1 .
- The mask of the sideway vehicle is represented by the e_3-e_4 basis vector, as shown in Fig. 7(b). Similarly, the physical meaning of the e_3 base vector represents the light ray direction of the sideway vehicle, and e_4 is the vertical vector of e_3 .

Figure 7 is transformed into the same coordinate system, and a 2D base vector geometric model is constructed as shown in Fig. 8. The base vector transformation of the

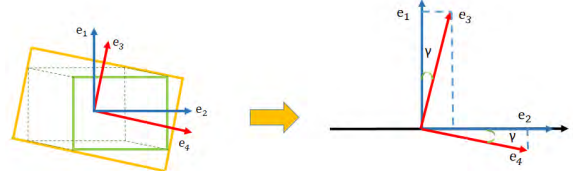


FIGURE 8. 2D base vector geometric model.

corresponding mask of the two types of vehicles is analyzed. The e_1-e_2 base vector is used as the baseline to observe the change of the e_3-e_4 base vector. The blue pair represents the base vector of the front vehicle, whereas the red pair represents the base vector of the sideway vehicle.

In accordance with its physical meaning, the angle (γ) of the offset between the base vectors is the local angle (θ_l). Given that the change in mask is consistent with the change in the base vector, Equation (2) can be obtained as follows:

$$\cos \gamma = \frac{|\mathbf{e}_1|}{|\mathbf{e}_3|} = \frac{|\mathbf{e}_1\mathbf{e}_2|}{|\mathbf{e}_3\mathbf{e}_4|} = \frac{S_{\text{front vehicle mask}}}{S_{\text{sideway vehicle mask}}}, \quad (2)$$

where $|\mathbf{e}_1\mathbf{e}_2|$ and $|\mathbf{e}_3\mathbf{e}_4|$ respectively represent the mask figures of the front and sideway vehicles. $S_{\text{front vehicle mask}}$ is the projected area of the front vehicle, whereas $S_{\text{sideway vehicle mask}}$ is the projected area of the sideway vehicle.

3) RELATIONSHIP BETWEEN THE ENTIRE MASK AND BACK MASK OF THE SIDEWAY VEHICLE

Given $\gamma = \theta_l$, $S_{\text{front vehicle mask}} = S_{\text{sideway vehicle back mask}}$, can obtain Equation (3).

$$\cos \theta_l = \frac{S_{\text{sideway vehicle back mask}}}{S_{\text{sideway vehicle mask}}} \quad (3)$$

From Equation (3), the relation between the entire mask of the sideway vehicle and the mask on the back of the sideway vehicle can be obtained, wherein the pixel value of the mask area is obtained from the segmentation information to represent the projected area.

D. DISTANCE ESTIMATION MODULE DESIGN

The projected area of the back of the vehicle obtained in the Section III-C.3 is combined with the actual vehicle dimensions and camera focal length (in pixels) for modeling based on the principle of camera projection to estimate the distance value of the vehicle ahead. Compared with the methods proposed in [2], [7], we use the perspective projection relationship between the actual and projected areas to establish the “area–distance” geometric model, which provides a more comprehensive use of vehicle information, to improve the accuracy of the distance estimation system. Moreover, we focus on the projection transformation relationship between surfaces, which can enhance the reliability of the geometric models compared with that in [8].

1) PRINCIPLE OF CAMERA PROJECTION

The principle of camera projection primarily transforms the points (X_w, Y_w, Z_w) in the world coordinate system into the

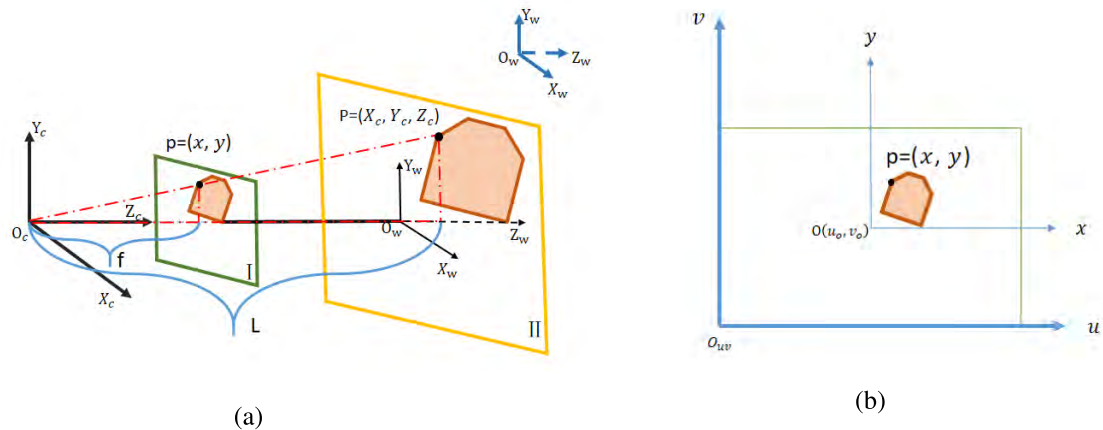


FIGURE 9. Projection geometry model of distance estimation, where f is the camera focal length and L is the physical distance between the object vehicle and the camera. (a) Principle of camera projection. (b) Image plane to pixel plane.

camera coordinate system (X_c, Y_c, Z_c) , which then become points (x, y) on the 2D plane through perspective projection. Lastly, the points (x, y) are stored in the form of pixels (u, v) , as shown in Fig. 9.

If the world coordinate system is in the position shown in Fig. 9(a), then $R = I$ (unit matrix), $T = [0 \ 0 \ L]^T$, $Z_w = 0$, and Equation (4) can be obtained.

$$\begin{bmatrix} X_c \\ Y_c \\ Z_c \\ 1 \end{bmatrix} = \begin{bmatrix} R & T \\ 0^T & 1 \end{bmatrix} \begin{bmatrix} X_w \\ Y_w \\ Z_w \\ 1 \end{bmatrix} = \begin{bmatrix} 1 & 0 & 0 & 0 \\ 0 & 1 & 0 & 0 \\ 0 & 0 & 1 & L \\ 0 & 0 & 0 & 1 \end{bmatrix} \begin{bmatrix} X_w \\ Y_w \\ 0 \\ 1 \end{bmatrix} \quad (4)$$

As shown in Fig. 9(b), the image coordinate system is converted to the pixel coordinate system, as shown in Equation (5).

$$\begin{bmatrix} u \\ v \\ 1 \end{bmatrix} = \begin{bmatrix} \frac{1}{d_x} & 0 & u_0 \\ 0 & \frac{1}{d_y} & v_0 \\ 0 & 0 & 1 \end{bmatrix} \begin{bmatrix} x \\ y \\ 1 \end{bmatrix} \quad (5)$$

Applying the camera projection principle, as shown in Equation (6), and the conversion relationship between the actual and pixel points in the camera coordinate system can be obtained, as shown in Equation (7).

$$Z_c \begin{bmatrix} x \\ y \\ 1 \end{bmatrix} = \begin{bmatrix} f & 0 & 0 & 0 \\ 0 & f & 0 & 0 \\ 0 & 0 & 1 & 0 \end{bmatrix} \begin{bmatrix} X_c \\ Y_c \\ Z_c \\ 1 \end{bmatrix} \quad (6)$$

$$Z_c \begin{bmatrix} u \\ v \\ 1 \end{bmatrix} = L \begin{bmatrix} u \\ v \\ 1 \end{bmatrix}$$

$$= \begin{bmatrix} \frac{1}{d_x} & 0 & u_0 \\ 0 & \frac{1}{d_y} & v_0 \\ 0 & 0 & 1 \end{bmatrix} \begin{bmatrix} f & 0 & 0 & 0 \\ 0 & f & 0 & 0 \\ 0 & 0 & 1 & 0 \end{bmatrix} \begin{bmatrix} R & T \\ 0^T & 1 \end{bmatrix} \begin{bmatrix} X_w \\ Y_w \\ Z_w \\ 1 \end{bmatrix}$$

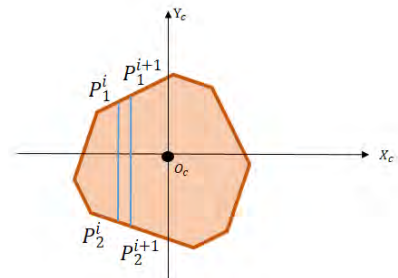


FIGURE 10. Actual area of the visible part of the target vehicle.

$$\begin{aligned} &= \begin{bmatrix} f_x & 0 & u_0 & 0 \\ 0 & f_y & v_0 & 0 \\ 0 & 0 & 1 & 0 \end{bmatrix} \begin{bmatrix} 1 & 0 & 0 & 0 \\ 0 & 1 & 0 & 0 \\ 0 & 0 & 1 & L \\ 0 & 0 & 0 & 1 \end{bmatrix} \begin{bmatrix} X_w \\ Y_w \\ 0 \\ 1 \end{bmatrix} \\ &= \begin{bmatrix} f_x & 0 & u_0 & u_0 L \\ 0 & f_y & v_0 & v_0 L \\ 0 & 0 & 1 & L \end{bmatrix} \begin{bmatrix} X_c \\ Y_c \\ 0 \\ 1 \end{bmatrix}, \end{aligned} \quad (7)$$

where $\frac{f}{d_x} = f_x$, $\frac{f}{d_y} = f_y$, $(u_0, v_0) = (0, 0)$, and $Z_c = L$, Equation (7) is transformed into Equation (8).

$$\begin{bmatrix} u \\ v \\ 1 \end{bmatrix} = \frac{1}{L} \begin{bmatrix} f_x X_c + u_0 L \\ f_y Y_c + v_0 L \\ L \end{bmatrix} = \frac{1}{L} \begin{bmatrix} f_x X_c \\ f_y Y_c \\ L \end{bmatrix} \quad (8)$$

2) RELATIONSHIP OF AREA CONVERSION IS DERIVED FROM THE RELATIONSHIP OF POINT CONVERSION

The actual area of the target vehicle is divided into N parts along the Y_c direction, and each part is approximately a rectangle, as shown in Fig. 10. The four vertices of the i -th rectangle are marked as P_1^i , P_1^{i+1} , P_2^i , and P_2^{i+1} , where $P_r^i = (P_{rx}^i, P_{ry}^i) = (x_r^i, y_r^i)$, ($r = 1, 2$; $i = 1, 2, 3, \dots, N$). P_{rx}^i and P_{ry}^i represent the X_c and Y_c coordinates of the four coordinate points, respectively.

Then, the actual area of the visible part of the target vehicle is

$$\begin{aligned} S &= \sum_{i=1}^N \left(P_{1y}^i - P_{2y}^i \right) \left(P_{2x}^{i+1} - P_{2x}^i \right) \\ &= \sum_{i=1}^N \left(y_1^i - y_2^i \right) \left(x_2^{i+1} - x_2^i \right). \end{aligned} \quad (9)$$

Using the relationship between the actual and pixel points (8), we can obtain

$$\begin{aligned} S &= \left[\sum_{i=1}^N \left(v_1^i - v_2^i \right) \left(u_2^{i+1} - u_2^i \right) \right] \frac{L^2}{f_x f_y} \\ &= S_{pixel} \frac{L^2}{f_x f_y}, \end{aligned} \quad (10)$$

where S_{pixel} represents the projected area of the target vehicle in the image, i.e., the pixel value of the mask formed by the projection of the vehicle in the image, and S represents the actual area of the vehicle.

3) ESTIMATE THE PHYSICAL DISTANCE OF THE VEHICLE AHEAD

In accordance with Equations (3) and (10), the distance formula (11) is obtained as

$$\begin{aligned} L &= \left(\frac{f_x f_y S}{S_{pixel}} \right)^{\frac{1}{2}} = \left(\frac{f_x f_y S_{sideway\ vehicle\ back}}{S_{sideway\ vehicle\ back\ mask}} \right)^{\frac{1}{2}} \\ &= \left(\frac{f_x f_y S_{sideway\ vehicle\ back}}{S_{sideway\ vehicle\ mask} \cos \theta_l} \right)^{\frac{1}{2}}, \end{aligned} \quad (11)$$

where L is the physical distance of the vehicle ahead $f_x = f_y = 7.2153 \times 10^2$, $S_{sideway\ vehicle\ back}$ is the actual area of the back of the sideway vehicle, and $S_{sideway\ vehicle\ mask}$ is the entire mask of the projected area of the sideway vehicle. θ_l is the local angle of the vehicle.

IV. EXPERIMENT

In this study, the proposed distance estimation system is mostly applied to the vehicle camera system in an automatic driving scene. The research scene is an actual traffic scene of a modern vehicle. The research device is a camera mounted behind the windshield of a vehicle for acquiring images.

We determine the vehicle's position on the basis of the definitions in the international vehicle collision warning system [29]. Vehicles ahead are divided into two types: the front and sideway vehicles. A front vehicle implies no deviation between the longitudinal center lines of the subject and target vehicles. If deviation exists, then the vehicle ahead is a sideway vehicle.

Segmentation Network: In this work, the state-of-the-art instance segmentation network, namely, Mask R-CNN, was used as the segmentation network, and the candidate regions of the target detection network were segmented at the pixel

TABLE 1. Average error of distance estimation by different methods (m).

Distance range	0-10m	10-20m	>20m
method[1]	0.74	1.77	6.52
method[31]	0.81	1.81	7.21
<i>ours</i>	0.38	0.85	2.17

¹This footnote shows m = meters.

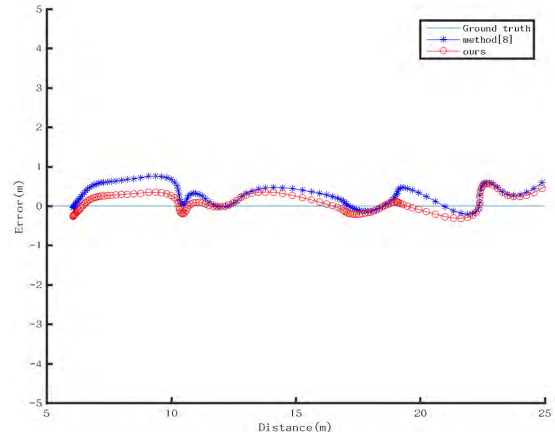


FIGURE 11. Absolute error curve graph.

level to obtain the mask that was used to calculate vehicle distance. Mask R-CNN has three advantages over Faster R-CNN. First, Mask R-CNN enhances the foundation of the network by using ResNeXt-101 with a feature pyramid network [28] as the feature extraction network. Second, Mask R-CNN replaces RoIPool with RoIAlign to solve the misalignment issues caused by the direct sampling of pooling. Third, Mask R-CNN can independently predict a binary mask for each class. The classification of each binary mask depends on the classification prediction given by the network region of interest (ROI) classification branch, and thus will not cause competition among classes. Mask R-CNN has demonstrated excellent performance in instance segmentation. Compared with the method represented by a 2D bounding box, a mask is used to obtain the details of the target vehicle, and the redundancy in the rectangle is reduced to improve the accuracy of the distance estimation system. Therefore, Mask R-CNN was selected as the segmentation network of our distance estimation system, which can obtain the segmentation information of the target vehicle in the image to ensure the accuracy of the system.

Angle Regression Network And Dimension Estimation Network: Given that the angle regression and dimension estimation networks are based on the CNN network framework, we use the same regression network structure to obtain the required vehicle parameters, i.e., training a deep CNN to regress the angle of the vehicle and its dimensions. In the KITTI dataset, vehicles, vans, trucks, and buses are under different categories, and the distribution of the object dimensions for category instances is low-variance and unimodal. For example, the dimension variance for vehicles and cyclists

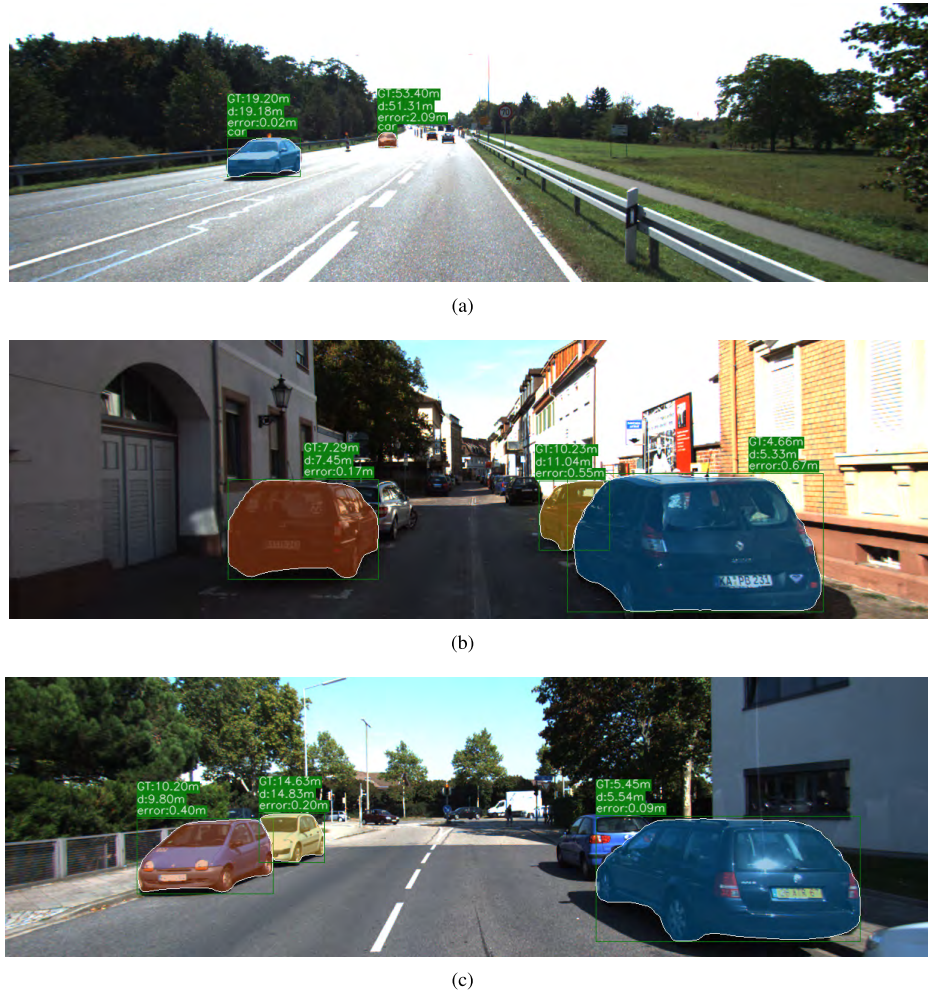


FIGURE 12. Distance experimental results on KITTI dataset.

is approximately several centimeters. Therefore, we use the L_2 loss directly. To regress vehicle parameters, we use a pre-trained VGG network [33] without its FC layers and add our angle and dimension estimation modules. During training, each ground truth crop is resized to 224×224 . To make the network more robust to viewpoint changes and occlusions, the ground truth boxes are jittered, and the ground truth angle is changed to account for the movement of the center ray of the crop.

Datasets: The networks involved in the distance estimation system proposed in this study are Mask R-CNN, ARN, and a dimension estimation network. We used the COCO and KITTI datasets [30] for training, thereby finally verifying our method on the KITTI detection benchmark. KITTI contains a training set of 7481 images and a test set 7518 images, and because our distance estimation system is for the automatic driving scene, it focuses only on the “car” category. The KITTI test dataset has no ground truth label. Following the “rules,” we separate a part of the data from the KITTI training set as a test set. The “rules” are as follows. First, the data of the training and test sets must be from

different video sequences. Second, the selected data should contain two scenarios: front and non-front. Third, ranging must be performed for vehicles with different distances. Thus, the selected verification image should include vehicle samples in different near and far situations. In accordance with this “rule,” we use the 3481 images in the training set as the test set to verify and analyze our distance estimation method.

Evaluation Metrics:

$$\begin{aligned}
 a. \text{Absolute Error} : \Delta(m) &= |L_{\text{ground truth}} - L_{\text{experimental}}| . \\
 b. \text{Relative Error} : \delta(\%) &= \left| \frac{\Delta}{L_{\text{ground truth}}} \right| . \\
 c. \text{Average Error} : \bar{\Delta}(m) &= \frac{1}{n} \sum_{i=1}^n |\Delta_i| . \\
 d. \text{Average Error Rate} : \bar{\delta}(\%) &= \frac{1}{n} \sum_{i=1}^n \left| \frac{\Delta_i}{L_{\text{ground truth}} i} \right| .
 \end{aligned}$$

To verify the accuracy and robustness of the proposed distance estimation system, we compared it with different dis-

TABLE 2. Comparison between experimental distance and ground truth of two groups of experiments.

	Number	1	2	3	4	5	6	7
Distance verification of front vehicles	Ground truth(m)	6.28	11.78	18.05	19.03	23.97	23.99	28.016
	Experimental distance(m)	6.39	12.01	18.22	19.19	24	23.91	28.17
	Absolute Error(m)	0.11	0.23	0.17	0.16	0.03	0.08	0.154
Distance verification of sideway vehicles	Ground truth(m)	5.45	7.68	10.84	11.06	13.395	19.205	53.395
	Experimental distance(m)	5.54	7.41	10.65	11.27	12.91	19.18	51.31
	Absolute Error (m)	0.09	0.27	0.19	0.21	0.485	0.025	2.085
The average error rate of distance estimates for Front vehicles and Sideway vehicles								
Method	Front vehicle's average error rate(%)				Sideway vehicle's average error rate (%)			
Method [32]	4.702				9.237			
Method [8]	1.333				4.698			
Ours	<u>1.077</u>				<u>2.820</u>			

tance estimation methods from three aspects, namely, accuracy verification of the entire system model, attitude angle module verification, and system robustness verification.

A. ACCURACY VERIFICATION OF THE ENTIRE SYSTEM MODEL

We compare the average error of the distance estimation results with the different methods proposed in [1] and [31], and the results are presented in Table 1. In the system framework of the methods presented in [1], [31], a “non-area-distance” geometric model was established by using the perspective principle to estimate distance, whereas we propose to use the area projection principle to establish the “area-distance” geometric model to realize distance estimation.

The experiment shows that the results of our method are optimal for distance estimation within different distance ranges. The average error of the estimation results using our distance estimation method is reduced by 0.43 m at the maximum compared with the other methods within the range of 10 m. Even within the range of distances greater than 20 m, the average error of our distance estimation results is guaranteed to be approximately 2 m. Compared with the methods proposed in [1], [31], the average error is considerably reduced, the optimal result is achieved, and the distance estimation accuracy of the system is improved. Moreover, the maximum deviation among the average errors over different distance ranges is approximately 1.8 m. Compared with the method presented in [31], the deviation between the system estimation results of different distances is reduced, and the overall distance estimation system is more stable and robust.

B. ATTITUDE ANGLE MODULE VERIFICATION

For the absolute error of different distance ranges, our method is compared with the method that disregards vehicle attitude angle information [8]. The method proposed in [8] is included in our test set, and the result is represented in the form of a curve graph, as shown in Fig. 11. In Fig. 11, the variation trend of errors within different distance ranges can be seen clearly. Our results at different distance positions present a slight deviation from the ground truth, and overall system accuracy and stability are improved.

To show the advantages of our system more intuitively, the result is illustrated in Fig. 12, thereby verifying the accuracy of the predicted values with the ground truth.

Figure 12 presents the visualization of our method for estimating the distance between the sideway and occluded vehicles. The results show that after adding the attitude angle information of the target vehicle in our distance estimation system framework, the absolute error of the target vehicle ranging result within 25 m is guaranteed to be less than 1 m. Even for target vehicles larger than 50 m, the absolute error can be guaranteed to be approximately 2 m.

C. SYSTEM ROBUSTNESS VERIFICATION

To evaluate the performance of the proposed method more comprehensively and verify the robustness of the system, front and sideway vehicles with different attitude angle information are used in testing. Meanwhile, the average error rate of the distance estimation results of different types of vehicles is compared with the methods proposed in [8] and [32]. The results are presented in Table 2.

On the basis of the experimental results, the average error rate of our method for estimating the distance of a sideway

vehicle is reduced to approximately 2.8%, thereby indicating a considerable decrease compared with other methods. Moreover, the deviation in the average error rate of the distance estimation results between the front and sideway vehicles is approximately 2%. The average error rate for the estimated distance results among different types of vehicles is substantially reduced compared with other methods, thereby overcoming the limitations and inapplicability of existing distance estimation methods.

V. CONCLUSION

This study combines the attitude angle information of a vehicle with its segmentation information and proposes a robust inter-vehicle distance estimation method from an in-car camera based on monocular vision. Considering the attitude angle changes of different types of vehicles in complex traffic scenarios, distance estimation based on angle information can improve the problem of considerable variation in the ranging accuracy of different types of vehicles, thereby solving the system problem of limited detection range, improving the robustness and accuracy of the system, helping drivers focus on the situation ahead, and reducing the occurrence of traffic accidents. From the experimental results, this method can adapt to most traffic scenarios and exhibits good robustness against different driving states of vehicles ahead.

In the future, we will analyze vehicles driving in different scenarios (such as highway, corner, and rural street scenes) to further expand our distance estimation system. In addition, for the front occlusion vehicle, there is no simple method with high accuracy and efficiency in the existing distance estimation methods. In order to improve the applicability of our method, we will focus on this aspect and continuously improve our distance estimation system.

REFERENCES

- [1] L.-C. Liu, C.-Y. Fang, and S.-W. Chen, "A novel distance estimation method leading a forward collision avoidance assist system for vehicles on highways," *IEEE Trans. Intell. Transp. Syst.*, vol. 18, no. 4, pp. 937–949, Apr. 2017.
- [2] J. Han, O. Heo, M. Park, S. Kee, and M. Sunwoo, "Vehicle distance estimation using a mono-camera for FCW/AEB systems," *Int. J. Automot. Technol.*, vol. 17, no. 3, pp. 483–491, Jun. 2016.
- [3] M. Rezaei, M. Terauchi, and R. Klette, "Robust vehicle detection and distance estimation under challenging lighting," *IEEE Trans. Intell. Transp. Syst.*, vol. 16, no. 5, pp. 2723–2743, Oct. 2015.
- [4] P. Wongsaree, S. Sinchai, P. Wardkein, and J. Koseyaporn, "Distance detection technique using enhancing inverse perspective mapping," in *Proc. 3rd Int. Conf. Comput. Commun. Syst. (ICCCS)*, Apr. 2018, pp. 217–221.
- [5] K. Nakamura, K. Ishigaki, T. Ogata, and S. Muramatsu, "Real-time monocular ranging by Bayesian triangulation," in *Proc. IEEE Intell. Vehicles Symp. (IV)*, Jun. 2018, pp. 1368–1373.
- [6] D. Bao and P. Wang, "Vehicle distance detection based on monocular vision," in *Proc. IEEE Int. Conf. Prog. Informat. Comput. (PIC)*, Dec. 2016, pp. 187–191.
- [7] D.-Y. Huang, C.-H. Chen, T.-Y. Chen, W.-C. Hu, and K.-W. Feng, "Vehicle detection and inter-vehicle distance estimation using single-lens video camera on urban/suburb roads," *J. Vis. Commun. Image Represent.*, vol. 46, pp. 250–259, Jul. 2017.
- [8] L. Huang, Y. Chen, Z. Fan, and Z. Chen, "Measuring the absolute distance of a front vehicle from an in-car camera based on monocular vision and instance segmentation," *J. Electron. Imag.*, vol. 27, no. 4, Jul. 2018, Art. no. 043019.
- [9] M. Hammer, M. Hebel, B. Borgmann, M. Laurenzis, and M. Arens, "Potential of lidar sensors for the detection of UAVs," *Proc. SPIE*, vol. 10636, pp. 10636-1–10636-7, May 2018.
- [10] J. Cui, F. Liu, Z. Li, and Z. Jia, "Vehicle localisation using a single camera," in *Proc. IEEE Intell. Vehicles Symp.*, Jun. 2010, pp. 871–876.
- [11] E. Raphael, R. Kiefer, P. Reisman, and G. Hayon, "Development of a camera-based forward collision alert system," *SAE Int. J. Passenger Cars-Mech. Syst.*, vol. 4, pp. 467–478, Apr. 2011.
- [12] D. O. Cualain, M. Glavin, E. Jones, and P. Denny, "Distance detection systems for the automotive environment: A review," in *Proc. Irish Signals Syst. Conf.*, 2007, pp. 13–14.
- [13] V. D. Nguyen, T. T. Nguyen, D. D. Nguyen, and J. W. Jeon, "Toward real-time vehicle detection using stereo vision and an evolutionary algorithm," in *Proc. IEEE 75th Veh. Technol. Conf. (VTC Spring)*, May 2012, pp. 1–5.
- [14] G. Kim and J.-S. Cho, "Vision-based vehicle detection and inter-vehicle distance estimation," in *Proc. IEEE Int. Conf. Control, Autom. Syst.*, Jeju Island, South Korea, Oct. 2012, pp. 17–21.
- [15] A. A. Ali and H. A. Hussein, "Distance estimation and vehicle position detection based on monocular camera," *Proc. Al-Sadeq Int. Conf. Multidisciplinary IT Commun. Sci. Appl. (AIC-MITCSA)*, 2016, pp. 1–4.
- [16] B. Li, X. Zhang, and M. Sato, "Pitch angle estimation using a vehicle-mounted monocular camera for range measurement," in *Proc. 12th Int. Conf. Signal Process. (ICSP)*, 2014, pp. 1161–1168.
- [17] S. Tuohy, D. O'Cualain, E. Jones, and M. Glavin, "Distance determination for an automobile environment using inverse perspective mapping in OpenCV," in *Proc. Signals Syst. Conf. (ISSC)*, Jul. 2010, pp. 100–105.
- [18] A. Bharade, S. Gaopande, and A. G. Keskar, "Statistical approach for distance estimation using inverse perspective mapping on embedded platform," in *Proc. Annu. IEEE India Conf. (INDICON)*, Dec. 2014, pp. 1–5.
- [19] W. Yao and U. Stilla, "Comparison of two methods for vehicle extraction from airborne LiDAR data toward motion analysis," *IEEE Geosci. Remote Sens. Lett.*, vol. 8, no. 4, pp. 607–611, Jul. 2011.
- [20] R. Adamshuk et al., "On the applicability of inverse perspective mapping for the forward distance estimation based on the HSV colormap," in *Proc. IEEE Int. Conf. Ind. Technol. (ICIT)*, Mar. 2017, pp. 1036–1041.
- [21] A. Joglekar, D. Joshi, R. Khemani, S. Nair, and S. Sahare, "Depth estimation using monocular camera," *Int. J. Comput. Sci. Inf. Technol.*, vol. 2, no. 4, pp. 1758–1763, 2011.
- [22] D. Eigen, C. Puhrsch, and R. Fergus, "Depth map prediction from a single image using a multi-scale deep network," in *Proc. Adv. Neural Inf. Process. Syst. (NIPS)*, 2014, pp. 2366–2374.
- [23] D. Eigen and R. Fergus, "Predicting depth, surface normals and semantic labels with a common multi-scale convolutional architecture," in *Proc. IEEE Int. Conf. Comput. Vis. (ICCV)*, Dec. 2015, pp. 2650–2658.
- [24] H. Fu, M. Gong, C. Wang, K. Batmanghelich, and D. Tao, "Deep ordinal regression network for monocular depth estimation," in *Proc. IEEE Conf. Comput. Vis. Pattern Recognit. (CVPR)*, pp. 2002–2011, Jun. 2018.
- [25] K. He, G. Gkioxari, P. Dollár, and R. Girshick, "Mask R-CNN," in *Proc. IEEE Int. Conf. Comput. Vis. (ICCV)*, Oct. 2017, pp. 2961–2969.
- [26] A. Mousavian, D. Anguelov, J. Flynn, and J. Kosecka, "3D bounding box estimation using deep learning and geometry," in *Proc. IEEE Conf. Comput. Vis. Pattern Recognit. (CVPR)*, Jul. 2017, pp. 7074–7082.
- [27] V. T. B. Tram and M. Yoo, "Vehicle-to-vehicle distance estimation using a low-resolution camera based on visible light communications," *IEEE Access*, vol. 6, pp. 4521–4527, 2018.
- [28] T.-Y. Lin, P. Dollár, R. Girshick, K. He, B. Hariharan, and S. Belongie, "Feature pyramid networks for object detection," in *Proc. IEEE Conf. Comput. Vis. Pattern Recognit. (CVPR)*, Jul. 2017, pp. 2117–2125.
- [29] Intelligent Transport Systems—Forward Vehicle Collision Warning Systems—Performance Requirements and Test Procedures, Standard ISO 15623:2013, Intelligent Transport Systems, 2013.
- [30] A. Geiger, P. Lenz, and R. Urtasun, "Are we ready for autonomous driving? The KITTI vision benchmark suite," in *Proc. IEEE Conf. Comput. Vis. Pattern Recognit. (CVPR)*, Jun. 2012, pp. 3354–3361.
- [31] S. Sivaraman and M. M. Trivedi, "Integrated lane and vehicle detection, localization, and tracking: A synergistic approach," *IEEE Trans. Intell. Transp. Syst.*, vol. 14, no. 2, pp. 906–917, Jun. 2013.
- [32] R. Garg, V.K. B.G., G. Carneiro, and I. Reid, "Unsupervised CNN for single view depth estimation: Geometry to the rescue," in *Computer Vision—ECCV*. Cham, Switzerland: Springer, 2016, pp. 740–756.
- [33] K. Simonyan and A. Zisserman. (2014). "Very deep convolutional networks for large-scale image recognition." [Online]. Available: <https://arxiv.org/abs/1409.1556>

- [34] S. Ren, K. He, R. Girshick, and J. Sun, "Faster R-CNN: Towards real-time object detection with region proposal networks," in *Proc. Adv. Neural Inf. Process. Syst. (NIPS)*, 2015, pp. 91–99.
- [35] C. Wang *et al.*, "Data provenance with retention of reference relations," *IEEE Access*, vol. 6, pp. 77033–77042, 2018.
- [36] C. Wang, Z. Zhao, L. Gong, L. Zhu, Z. Liu, and X. Cheng, "A distributed anomaly detection system for in-vehicle network using HTM," *IEEE Access*, vol. 6, pp. 9091–9098, 2018.
- [37] S. Liu, Z. Li, Y. Zhang, and X. Cheng, "Introduction of key problems in long-distance learning and training," *Mobile Netw. Appl.*, vol. 24, no. 1, pp. 1–4, 2019.
- [38] W.-D. Xie and X. Cheng, "Imbalanced big data classification based on virtual reality in cloud computing," 2019. doi: [10.1007/s11042-019-7317-x](https://doi.org/10.1007/s11042-019-7317-x).
- [39] M. P. Deisenroth, A. A. Faisal, and C. S. Ong, *Mathematics for Machine Learning*. Cambridge, U.K.: Cambridge Univ. Press, 2018, pp. 1541–1911. [Online]. Available: <https://mml-book.com>



LIQIN HUANG received the Ph.D. degree from Fuzhou University, Fuzhou, China, where he is currently a Full Professor with the College of Physics and Information Engineering. His research interest include image processing, computer vision, artificial Intelligence, traffic scene understanding, and medical image processing.



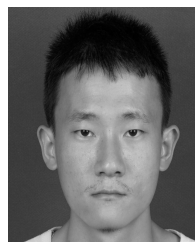
TING ZHE received the B.S. degree in electronic information science and technology from Shenyang Ligong University, Shenyang, China, in 2017. She is currently pursuing the M.S. degree in electronics and communications engineering with Fuzhou University, Fuzhou, China. Her current research interests include image processing, computer vision, and deep learning.



JUNYI WU received the B.S. degree in electronic information engineering from the Xiamen University of Technology, Fujian, China, in 2017. He is currently pursuing the M.S. degree with Fuzhou University. His research interests include computer vision and deep learning.



QIANG WU (SM'18) received the B.Eng. and M.Eng. degrees from the Harbin Institute of Technology, Harbin, China, in 1996 and 1998, respectively, and the Ph.D. degree from the University of Technology Sydney, Ultimo, NSW, Australia, in 2004. He is currently an Associate Professor and a Core Member of the Global Big Data Technologies Center, University of Technology Sydney. His research has been published in many premier international conferences, including ECCV, CVPR, ICIP, and ICPR, and major international journals, such as TIP, TSMCB, TCSV, and TSP. His research interests include computer vision, image processing, pattern recognition, machine learning, and multimedia processing. He serves as a Reviewer for several journals, including TPAMI, TIP, TCSV, and TSMCB.



CHENHAO PEI received the B.S. degree in internet of things engineering from Fuzhou University, Fujian, China, in 2016, where he is currently pursuing the Ph.D. degree in communication and information system. His research interests include lane detection, deep learning, autonomous driving, and computer vision.



DAN CHEN received the M.S. degree in signal and information processing from Fuzhou University, China, in 2011, where he is currently a Lecturer with the College of Physics and Information Engineering. His current research interest includes computer vision, machine learning, and edge computing.

• • •